MedChemComm

Accepted Manuscript

This is an *Accepted Manuscript*, which has been through the Royal Society of Chemistry peer review process and has been accepted for publication.

Accepted Manuscripts are published online shortly after acceptance, before technical editing, formatting and proof reading. Using this free service, authors can make their results available to the community, in citable form, before we publish the edited article. We will replace this *Accepted Manuscript* with the edited and formatted *Advance Article* as soon as it is available.

You can find more information about *Accepted Manuscripts* in the Information for Authors.

Please note that technical editing may introduce minor changes to the text and/or graphics, which may alter content. The journal's standard Terms & Conditions and the Ethical guidelines still apply. In no event shall the Royal Society of Chemistry be held responsible for any errors or omissions in this *Accepted Manuscript* or any consequences arising from the use of any information it contains.

ROYAL SOCIETY OF CHEMISTRY

www.rsc.org/medchemcomm

Journal Name

ARTICLE

Drug trapping in hERG K$^+$ channels: (not) a matter of drug size?‡

Tobias Linder[a]†, Harald Bernsteiner[a]†, Priyanka Saxena[a]†, Florian Bauer[b], Thomas Erker[b], Eugen Timin[a], Steffen Hering[a], A. Stary-Weinzinger[a*]

Received 00th January 20xx,
Accepted 00th January 20xx

DOI: 10.1039/x0xx00000x

www.rsc.org/

Inhibition of hERG K$^+$ channels by structurally diverse drugs prolongs the ventricular action potential and increases the risk of torsade de pointes arrhythmias and sudden cardiac death. Capture of drugs behind closed channel gates, so-called drug trapping, is suggested to harbor an increased pro-arrhythmic risk. In this study the trapping mechanism of the trapped hERG blocker propafenone and a bulky derivative (MW: 647.24 g/mol) were studied by making use of electrohysiological measurements in combination with molecular dynamics simulations. Our study suggests that the hERG cavity is able to accommodate very bulky compounds without disturbing gate closure.

Introduction

hERG K$^+$ channels (Kv11.1) are critical for the repolarization of the cardiac ventricular action potential and thus are essential for the regulation of a normal electrical heart rhythm.[1] Loss of channel function, due to inherited mutations,[2] or more commonly due to unwanted binding of small molecules,[3] can lead to long QT intervals. In the worst case this channel malfunction can cause deadly arrhythmia.[4] These 'off-target' effects led to intense efforts devoted towards understanding how drug molecules physical bind to and block the pore of the hERG channel to reduce K$^+$ ion flux.[5]

It was proposed that many drugs that block hERG can become trapped within the central cavity, when the activation gate closes due to membrane repolarization.[6–10] This phenomenon, referred to as 'drug-trapping', can explain why certain drugs cannot be washed off when channels are held in a closed state.[11] Strong evidence for drug trapping came from studies with a mutant D540K, which can reopen at hyperpolarized membrane potentials, enabling almost complete recovery of otherwise trapped compounds.[6]

Trapping is not unique to hERG K$^+$ channels, but was first described for quaternary ammonium (QA) blockers by Armstrong in 1971.[12] We have previously provided insights into the structural mechanisms of trapping of a medium size (MW: 242.46 g/mol) QA blocker. Our atomistic molecular dynamics simulations provided insights into the dynamics of the trapping process for tetrabutylammonium (TBA) in hERG K$^+$ channels. Our simulations proposed that trapping can influence the dynamics of the high affinity binding determinant F656. In particular, our simulations suggested that F656 presents a physical barrier for drug dissociation of TBA. Further our simulations revealed that drug trapping of this compound does not influence the closure mechanism per se, nor does it change the structure of the gate.[13]

It was previously suggested for other K$^+$ channels that larger compounds might disrupt closure of the activation gate, while not really becoming trapped within the central cavity. This mechanism was termed 'foot in the door'.[12] This phenomenon was first described by Armstrong in 1971, where it was shown that trapping correlated with the size of QA blockers. While smaller molecules fitted into the cavity, larger QA compounds were unable to be trapped and had to dissociate before deactivation, presumably due to limited cavity size.[12]

The hERG K$^+$ channel cavity is rather unique, since it is able to bind many structurally diverse chemicals of various size with high affinity.[5] In order to investigate if larger compounds influence or prevent proper channel closure in hERG, we made use of the well-studied class Ic antiarrhytmic drug propafenone,[14] which is known to be trapped in the hERG channel[8] and synthesized a novel bulky derivative (Fig. 1A). By combining two-electrode voltage clamp analysis and molecular dynamics simulations we provide detailed insights into drug trapping in relation to compound size in hERG channels.

[a] Department of Pharmacology and Toxicology, University of Vienna, Austria.
[b] Department of Pharmaceutical Chemistry, University of Vienna, Austria.

† contributed equally. * Correspondence to: anna.stary@univie.ac.at
‡ The authors declare no competing interests.
See DOI: 10.1039/x0xx00000x

Methods

Synthesis of 1-[2-[2-Hydroxy-3-[4-tritylpiperazin-1-yl)-3-phenylpropan-1-on (FB213)

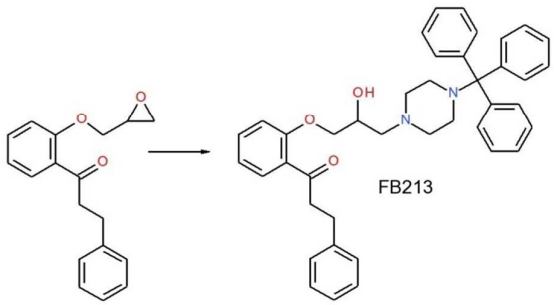

1-[2-(Oxiran-2-ylmethoxy) phenyl]-3-phenyl-propan-1-one

All chemicals obtained from commercial suppliers were used as received and were of analytical grade. Melting points were determined on a Kofler hot stage apparatus and are uncorrected. The 1H- and 13C-NMR spectra were recorded on a Bruker Avance DPx200 (200 and 50 MHz).

Synthesis of FB213: 1-[2-[2-Hydroxy-3-[4-tritylpiperazin-1-yl)-3-phenylpropan-1-on

A mixture of 1-[2-(Oxiran-2-ylmethoxy)phenyl]-3-phenyl-propan-1-one (0.576 g, 2.04 mmol] and 1-tritylpiperazine [0.688 g, 2.09 mmol]) in 2-propanol was heated to reflux for 6 hours. Upon completion of the reaction the solvent was evaporated and the residue was recrystallized from ethyl acetate to obtain title compound as a white solid (yield: 0.854 g, 68.5%).

The analysis of this material gave the following results: Mp 162 - 165°C; 1H-NMR (CDCl3): 7.78 - 7.65 (m, 1H), 7.58 - 7.10 (m, 21H), 7.05 - 6.85 (m, 2H), 4.18 - 3.81 (m, 3H), 3.58 - 2.20 (m, 10H), 1.60 (s-br, 2H); 13C-NMR (CDCl3): 201.4, 158.0, 141.8, 133.6, 130.6, 129.5, 128.5, 128.3, 127.7, 126.2, 126.0, 121.1, 112.7, 77.0, 70.9, 65.2, 61.0, 47.9, 45.9, 30.4. MS m/z 411 [0.1%], 125 [13%], 99 [100%]. Anal.Calcd for C41H42N2O3: C, 80.62; H, 6.93; N, 4.59. Found: C, 80.41; H, 6.83; N, 4.55.

Electrophysiology

cDNAs of hERG (accession number NP000229) was kindly provided by Prof. Sanguinetti (University of Utah, UT, USA). Synthesis of capped runoff complementary ribonucleic acid (cRNA) transcripts from linearized cDNA (cDNA) templates and injection of cRNA were performed as described in detail by Sanguinetti et al.[2] Oocytes from the South African clawed frog, Xenopus laevis (NASCO, Fort Atkinson, WI, USA), were prepared as follows: After 15 min exposure of female Xenopus laevis to the anesthetic (0.2% solution of MS-222; the methanesulfonate salt of 3-aminobenzoic acid ethyl ester; Sigma), parts of the ovary tissue were surgically removed. Defolliculation was achieved by enzymatical treatment with 2 mg/mL collagenase type 1A (Sigma) and mechanical removal of follicular layer using forceps. Stage V–VI oocytes were selected and injected with the WT and mutant hERG-encoding cRNA. Injected oocytes were stored at 18 °C in ND96 bath solution (96 mM sodium chloride, 2 mM potassium chloride, 1 mM magnesium chloride, 5 mM HEPES, 1.8 mM CaCl2; pH 7.5, titrated with NaOH) containing 1% penicillin-streptomycin solution. All chemicals used were purchased from Sigma-Aldrich Chemie GmbH, Taufkirchen, Germany.

Currents through hERG channels were studied 1 to 4 days after microinjection of the cRNA using the two-microelectrode voltage clamp technique. ND96 was used as extracellular recording solution. Voltage-recording and current-injecting microelectrodes were filled with 3 M KCl and had resistances between 0.3 and 2 MΩ. Endogenous currents (estimated in oocytes injected with DEPC water) did not exceed 0.15 µA. Currents >5 µA were discarded to minimize voltage clamp errors. Ionic currents were recorded with a Turbo Tec 03X Amplifier (npi electronic, GmbH, Tamm, Germany) and digitized with a Digidata 1322A (Axon Instruments Inc., Union City, CA, USA). The pClamp software package version 9.2 (Axon Instruments Inc.) was used for data acquisition. Microcal Origin 7.0 was employed for analysis and curve fitting.

A precondition for all measurements was the achievement of stable peak current amplitudes over periods of 10 min after an initial run-up period. A frequency of 0.3 Hz was used for all voltage clamp experiments. Drugs were applied by means of a perfusion system enabling solution exchange within 100 ms[26]. Control measurements for 30-35 minutes after an initial 'run up' phase were performed and no significant changes in current amplitude were observed. The flow rate was ≈ 8 µl/s preventing run down during experiments (data no shown). The oocytes were kept for 5 min at a holding potential of −100 mV to equilibrate drug diffusion. The tail current was measured at −50 mV, after a step to +20 mV. Use-dependent hERG channel block was estimated as peak tail current inhibition. Data are presented as means ± s.e. from at least four oocytes from ≥2 batches. The studied compound FB213 was dissolved in ND96 extracellular recording solution to prepare a 10 µM stock on the day of experiments. Drug stock solution was further diluted to the required concentration.

Molecular docking

The hERG homology model, termed "model 6" from our recently published analysis of structural hERG models was used for docking.[18] Modeling procedures and validation are described in detail in our previous paper. Briefly, Modeller 7v7[29] was used to generate a 3D model of the open conformation of hERG1. Based on the crystal structure of KvAP[30] and a refined model thereof.[31]

Docking was performed using the program Gold 4.0.1 and the implemented Gold scoring function. The binding site was defined by selecting Y652 and F656 of all four subunits as center and including all residues within a radius of 10 Å of these two residues. The

rotameric state of the aromatic side chains was set to library taking into account side chain flexibility.[15] For both drugs the central nitrogen was protonated and used in charged form. The 20 best-ranked poses of each drug docking run were visually inspected and the most frequent binding mode was used as starting conformation for ED simulations. General amber force field parameters[16] for the drugs were generated by making use of Gaussian 09[27] and antechamber.[28]

Essential Dynamics Simulations (ED)

The ED technique was described previously.[17] Briefly, an eigenvector representing the transition between open and closed hERG channel states was obtained from a principal component analysis, by comparing the backbone atoms of both states. The fixed increment linear expansion method was used and set to $-1.69e^{-6}$ nm per simulation step (2 fs). Five closing ED simulations, each lasting 20 ns, were performed in the presence of propafenone and FB213, respectively. Data for apo simulations were taken from our previous publication.[13]

Results and discussion

FB213 inhibits hERG currents and is trapped in the cavity

hERG channels were expressed in *Xenopus laevis* oocytes and K^+ current was measured using the standard two-electrode voltage clamp technique. A two-step pulse protocol was applied (Fig. 1B): 300 ms depolarization to +20 mV (prepulse) induces slow activation and fast inactivation of the channels, potassium current during prepulse is small. Upon repolarization to −50 mV, channels undergo rapid recovery from inactivation inducing large "tail" currents and slowly deactivate (closure of the channel gate). Peak tail current amplitudes were used as a measure of fraction of channels free from drug inhibition. First, we determined the sensitivity of FB213 to WT hERG channels. The concentration inhibition relationship was estimated by plotting the steady state values of current inhibition normalized to control (in drug free solution) versus cumulatively applied FB213 concentrations (Fig. 1C and D). The concentration of FB213 required to block 50 % (IC_{50}) of the hERG current was 47.1 ± 5.1 µM. The oocyte was exposed to drug and after 5 min of equilibration a train of pulses (with frequency of 1 Hz) was applied inducing "use dependent" inhibition of hERG channels (Fig.1F, block): peak tail currents were gradually decreased and finally reached a steady state.

State-dependent block was measured in the absence of FB213 (control, Fig. 1E) and after a pre-incubation period of 330 s with 150 µM FB213 (3 x IC_{50}) while holding the channels at −100 mV. Subsequently, 1 Hz pulse trains were applied until steady state block was reached. Channel block developed in a 'use-dependent' manner. Prepulse and tail currents were inhibited during the 1 Hz pulse train. The steady state block was achieved within 15 s (Fig. 1E green trace and 1F). The development of block during channel activation at +20 mV suggests that FB213 blocks hERG channels in an open channel conformation. 150 µM FB213 blocked hERG channels by 69 ± 5% (Fig. 1F).

Further, we probed if FB213 is trapped inside the hERG cavity. The criteria of drug trapping in hERG channel cavity are: i) lack of recovery from block at rest and ii) slow recovery and acceleration of recovery during washout of the drug.[9] Recovery from hERG channel block by FB213 was determined by applying a test pulse after a resting period of 300 s at holding potential of −100 mV, where the channels are in a closed resting state. The first current amplitudes after this rest period recovered from block less than 1%, indicating that FB213 is trapped in the closed channel conformation (Fig. 1E red trace and 1F). Previously it has been demonstrated that hERG channels inhibited by "non-trapped" drugs recover during ≈ 330 s even in presence of drug.[9,10] Subsequent frequent opening of the channel at 0.3 Hz, during wash out induced substantial recovery from FB213 block to 47.5 ± 3.7 % (Fig. 1E blue trace and 1G) suggesting that trapped FB213 can leave the channel during activation when the channels are in an open conformation.

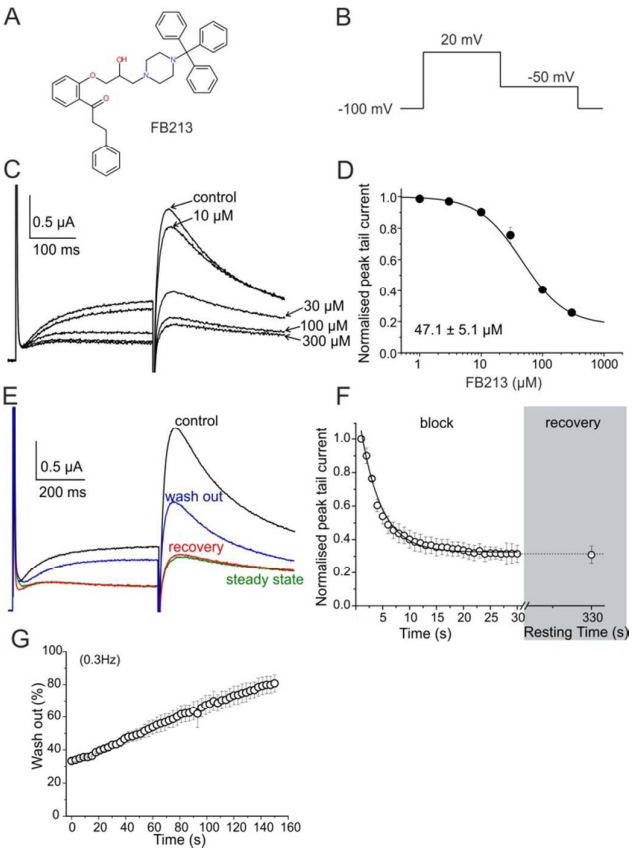

Fig. 1 WT hERG channels inhibition by Fb213. (A) chemical structure of FB213, (B) voltage pulse protocol shown; (C) superimposed current traces recorded in the absence (control) and after attaining steady-state block with increasing concentrations of FB213 at 0.3 Hz; (D) the

concentration-response relationship for the block of hERG tail current by FB213; (E) superimposed current traces of first (control, black) and last ('steady-state block', green) pulse during a conditioning train of 1 Hz, after application of 150 µM FB213. Recovery current from FB213 block in the continued presence of drug at rest, resulting from a single test pulse after 330 s resting time is depicted as red, washout of FB213 block is shown in blue; (F) mean normalized peak tail current amplitudes in the presence of 150 µM FB213 is plotted against time. The section 'block' shows the development of inhibition during a 1 Hz pulse train. The grey highlighted section 'recovery' maps the amount of recovery after a 330 s resting time; (G) repetitive stimulation accelerates wash-out of FB213. hERG channels were inhibited by a 1 Hz pulse train, as described in Fig. 1F. After reaching steady state of inhibition, the drug was washed out. During the wash-out process, pulses were applied at 0.3 Hz frequency. Peak tail currents were normalized to control currents (amplitude before drug application) and plotted against time.

To test if FB213 binds to the central cavity, as shown previously for other propafenone derivatives[10] we performed alanine mutation studies on Y652 and F656, which have been shown to play a key role for binding of different chemical entities.[6] The WT channel voltage protocol was utilized for Y652A, while tail currents were measured at −140 mV for F656A as reported by Witchel et al.[8] Y652A and F656A significantly reduced channel inhibition to 13.2 ± 4.4 % and 18.3 ± 1.2 %, respectively (Fig. 2A–C) suggesting that FB213 not only can access the binding site inside the cavity, but further interacts with Y652 and F656, as shown for many well-known hERG blockers.

Taken together, these results suggest that FB213 can bind to the well-established receptor site, located deeply in the channel pore and does not dissociate from the channel at rest. Washing out provided negligible recovery from block which is prominently enhanced by frequent stimulation.

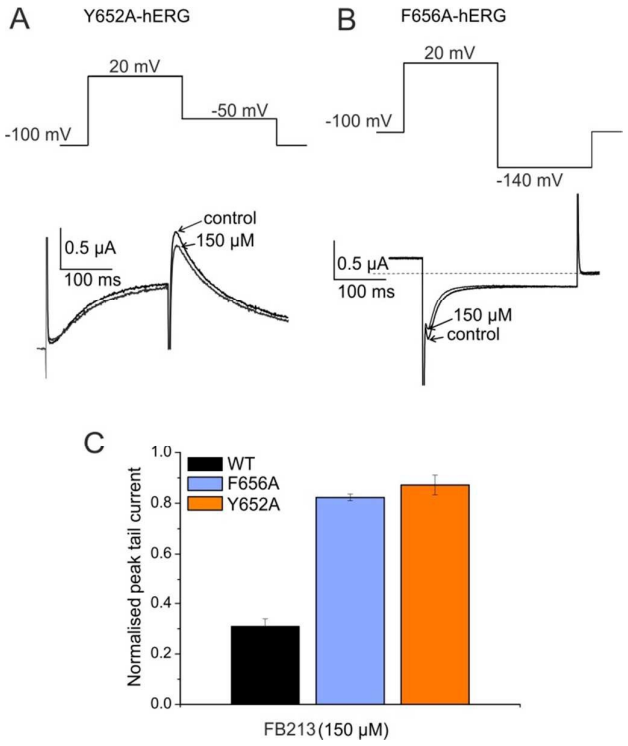

Fig. 2 FB213 interacts with binding site Y652 and F656. (A, B). Representative current traces and corresponding voltage protocols for current measurements of mutants Y652A and F656A in the absence (control) and presence of FB213 respectively. Tail currents of F656A were recorded at −140 mV; (C) Normalized peak tail currents of WT, Y652A, and F656A channels after steady state block by 150 µM FB213 (n = 4, error bars, ± SEM).

Structural investigation of FB213 Block in hERG

To investigate the binding mode of FB213, we docked the compound into our previously published open state hERG homology model[18]. Hydrogen bonds between two adjacent hydroxyl groups of Y652 and the drug were observed. The protonated nitrogen of FB213 is located beneath the selectivity filter, stabilized by helix dipole charges and a hydrogen bond to Y652. The triphenyl moiety of the compound forms hydrophobic and aromatic interactions with two adjacent Y652 side chains and one F656 residue. As illustrated in Fig. 3B, multiple hydrophobic and aromatic interactions between the compound and the side chains of Y652 and F656 were observed (see also Table 2). This is in agreement with our experimental observations.

For comparison reasons we included the well-studied smaller propafenone (MW: 341.44 g/mol) compound in our ED investigations as well. As a starting point the molecule was docked into the open state, similar as FB213. Interactions are illustrated in Figure 4B. In agreement with experiment and previous docking studies[8,19] aromatic and hydrophobic interactions between propafenone and F656 and Y652 were

observed. Additionally, a hydrogen bond between the basic nitrogen and S624 was seen.

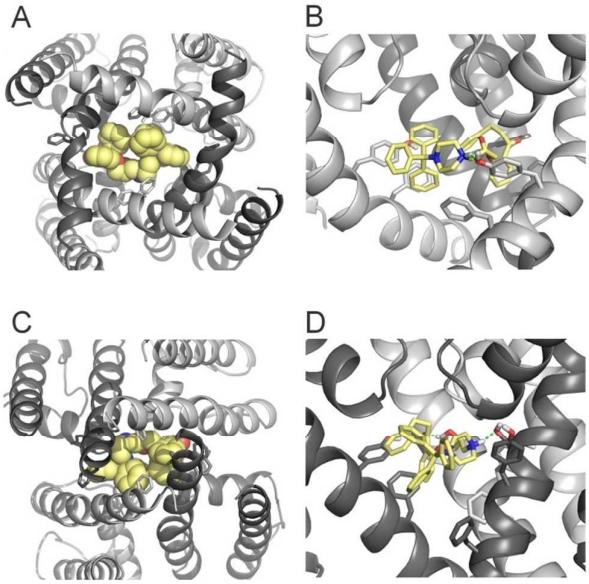

Fig. 3 Modelling of FB213 trapping. (A) Bottom view of FB213 (yellow spheres) docked into the open state hERG model. (B) side view of FB213 interactions with aromatic side chains of Y652 and F656. Hydrogen bonds are depicted as green dotted lines. (C) Bottom view of the trapped FB213 after 20 ns ED simulations. (D) Side view of the compound in the closed state.

Trapping simulations with propafenone and FB213

To investigate if propafenone and FB213 can indeed physically become trapped behind the activation gate, we performed five independent essential dynamics (ED) gating simulations with both drugs, respectively. The ED method was previously successfully applied by our group to investigate activation/deactivation gating in KcsA[17] and to monitor drug trapping of TBA in KcsA and hERG.[13] In a first step we compared the backbone atoms of the open and closed state hERG homology models by principal component analysis. The resulting eigenvector was then used to enforce channel closure, while leaving all other degrees of freedom essentially unbiased. The simulations enabled us to monitor drug trapping in atomistic detail on the nanosecond timescale. Closure of the activation gate was monitored by calculating the RMSD (root mean square deviation) of the protein compared to the closed state homology model. As shown in Table 1, the RMSD value decreased steadily, reaching minima between 2.33 and 3.51 Å. The somewhat higher RMSD values in two closing simulations (3.51 Å and 3.13 Å) resulted from unwinding of the helix termini. However, this was not influenced by the bound drug molecule, since the binding site was higher up in the cavity (see Figure 3A-D). Successful trapping was defined by a decrease of the RMSD and visual inspection of the gating region formed by S6 segments. As listed in Table 1 all 10 closing runs with the drugs were successful. Our ED simulations repeatedly show that the activation gate can close normally with FB213 as illustrated in Fig. 3C and D.

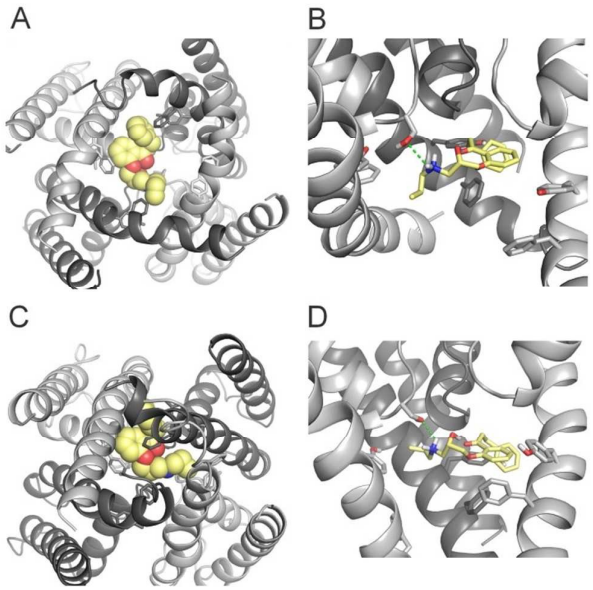

Figure 4. Modelling of propafenone trapping. (A) Bottom view of propafenone shown in yellow spheres representation docked into the open state hERG model. (B) Side view of propafenone interactions with the side chains of Y652, F656 and S624. Hydrogen bonds are depicted as green dotted lines. (C) Bottom view of the trapped propafenone molecule after 20 ns ED simulations. (D) Side view of the compound in the closed state.

Table 1 Analysis of closing simulations. Minimal root mean square deviation (MinRMSD) and time to reach the closed state are listed.

Closing simulations					
FBA213		Apo		Propafenone	
MinRMSD (Å)	Time (ns)	MinRMSD (Å)	Time (ps)	MinRMSD (Å)	Time (ns)
3,13	16,2	2,90	15,2	2,81	19,7
2,33	18,4	2,92	14,5	2,79	18,9
3,07	9,7	3,41	10,7	3,51	8,3
2,74	13,2	3,15	14,2	2,38	18,0
2,62	14,9	2,62	18,7	2,79	16,7

Since we have previously found that closure with a bound drug molecule can influence the dynamics of the F656 side chain,[13] we monitored the rotameric states of this residue during closure simulations. As shown in Fig. 5, propafenone as well as FB213 influence the dynamics of the side chain. In particular the bound propafenone stabilizes the down state of F656, which is defined as $\chi 1$ angles < -123°. Only at the end of the simulation the side chain of 1 subunit is found in the up-state ($\chi 1$ > -123°). These effects are similar as observed for TBA trapping in our previous study.[13] The situation is different for FB213. Due to the large size of this molecule, the behaviour of the F656 side chain is influenced. Already at the start, only two F656 side chains are able to adopt a down-conformation, while

the other two side chains have to adopt an 'up-ward' conformation. In all five closing simulations this distribution of F656 rotameric states does not change during closure. (Fig. 5)

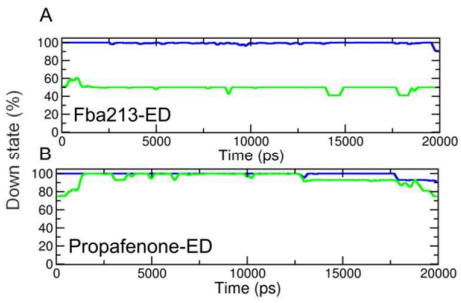

Figure 5. Analysis of rotameric states of F656. (A-B) Down states are defined by $\chi 1$ angles < -123°. The percentage of the down state was calculated for each time step and plotted over time averaged over 5 trapping runs/drug.

During channel closure the interactions between FB213 and the protein increase, compared to the observed open state interactions (Table 2). Due to rotation of the S6 helix during closure the side chain of S649 is reoriented, enabling hydrogen bonds with the protonated nitrogen, additionally to the OH-group of Y652 as shown in Fig. 3B and D. The location of the tertiary amine is only slightly different from the open state. This is in contrast to a previous docking study, which suggested that the basic nitrogen might move upward during channel closure.[19]

During channel closure with propafenone no major changes in interactions compared to the open state were observed (Figure 4B and D). Again the location of the basic nitrogen remained centrally, below the selectivity filter, stabilized by helix dipole charges. As expected due to size differences, the buried solvent accessible surface areas of FB213 compared to propafenone is considerably higher, as shown in Table 2. Interestingly, in ED run 2, propafenone did not displace any solvent from the surface areas of the protein. In this run the ligand is forming a U-shaped conformation. This is in agreement with a recent study by Schmidtke et al,[20] suggesting that drug interactions can become more favourable when the cavity size is decreased. During channel closure we often observe 2-fold symmetry, irrespective of the drug bound. This is also in line with closure simulations performed recently on hERG homology models without drug molecules.[20]

Table 2 – Analysis of ligand buried solvent accessible surface area. Calculations were performed with Surface Racer 5.0.[32]

buried solvent accessible surface areas (Ångström²)			
	total buried area	polar	non-polar
FB213			
run 1	450,17	130,3	319,86
run 2	414,16	104,08	310,09
run 3	443,52	128,47	315,05
run 4	408,39	117,35	291,06
run 5	456,21	126,36	329,84
average buried SASA	434,49	121,312	313,18
Propafenone			
run 1	212,9	80,04	132,87
run 2	1,12	0,35	0,77
run 3	203,11	30,91	172,21
run 4	382,15	112,82	269,33
run 5	258,01	94,4	163,59
average buried SASA	211,45	63,70	147,75

It is remarkable that a molecule of the size of FB213 seems to be accommodated in the hERG cavity without any difficulties. This suggests that the cavity of hERG is quite different from other potassium channels with smaller cavities, such as Shaker.[21] This underlines the uniqueness of the hERG cavity in terms of size and possibly plasticity, which has recently been recognized to play a major role in drug block as well.[15,20,22,23] It is conceivable that the hERG cavity might be able to accommodate even larger/bulkier molecules, when considering hydrophobic side pockets, which have been recently suggested to be accessible for drug interactions.[20,22,24] Interestingly, such a possibility has recently also been shown for a QA blocker in the bacterial K^+ channel KcsA.[25]

Conclusions

Our data suggests that pore blockers of different bulkiness may serve as tools to probe the size of the HERG cavity.
We found that even large blockers do not hinder normal gate closure. This indicates that the cavity of the hERG pore is remarkably large, enabling trapping of compounds with very high molecular weight (FB213: 647.24 g/mol). Further, we propose that for a propafenone like scaffold, size does not play a major role during drug trapping in hERG K^+ channels. Further studies will reveal if this holds true for structurally unrelated trapped drugs in hERG.

Acknowledgements

This work was supported by the Austrian Science Fund (FWF; grants P22395 and W1232; http://www.fwf.ac.at) and the Wiener Hochschuljubiläumsstiftung (grant H-304013/2014). The computational results presented have been achieved using the Vienna Scientific Cluster (VSC).

References

1 M. C. Sanguinetti and M. Tristani-Firouzi, *Nature*, 2006, **440**, 463–469.
2 M. C. Sanguinetti, C. Jiang, M. E. Curran and M. T. Keating, *Cell*, 1995, **81**, 299–307.
3 W. Haverkamp, G. Breithardt, A. J. Camm, M. J. Janse, M. R. Rosen, C. Antzelevitch, D. Escande, M. Franz, M. Malik, A. Moss and R. Shah, *Cardiovasc. Res.*, 2000, **47**, 219–233.
4 M. T. Keating and M. C. Sanguinetti, *Cell*, 2001, **104**, 569–580.
5 J. I. Vandenberg, M. D. Perry, M. J. Perrin, S. A. Mann, Y. Ke and A. P. Hill, *Physiol. Rev.*, 2012, **92**, 1393–1478.
6 J. S. Mitcheson, J. Chen and M. C. Sanguinetti, *J. Gen. Physiol.*, 2000, **115**, 229–240.
7 M. Perry, M. J. de Groot, R. Helliwell, D. Leishman, M. Tristani-Firouzi, M. C. Sanguinetti and J. Mitcheson, *Mol. Pharmacol.*, 2004, **66**, 240–249.
8 H. J. Witchel, C. E. Dempsey, R. B. Sessions, M. Perry, J. T. Milnes, J. C. Hancox and J. S. Mitcheson, *Mol. Pharmacol.*, 2004, **66**, 1201–1212.
9 D. Stork, E. N. Timin, S. Berjukow, C. Huber, A. Hohaus, M. Auer and S. Hering, *Br. J. Pharmacol.*, 2007, **151**, 1368–1376.
10 A. Windisch, E. Timin, T. Schwarz, D. Stork-Riedler, T. Erker, G. Ecker and S. Hering, *Br. J. Pharmacol.*, 2011, **162**, 1542–1552.
11 E. Carmeliet, *Circ. Res.*, 1993, **73**, 857–868.
12 C. M. Armstrong, *J. Gen. Physiol.*, 1971, **58**, 413–437.
13 T. Linder, P. Saxena, E. Timin, S. Hering and A. Stary-Weinzinger, *J. Chem. Inf. Model.*, 2014.
14 C. Funck-Brentano, H. K. Kroemer, J. T. Lee and D. M. Roden, *N. Engl. J. Med.*, 1990, **322**, 518–525.
15 K. Knape, T. Linder, P. Wolschann, A. Beyer and A. Stary-Weinzinger, *PloS One*, 2011, **6**, e28778.
16 J. Wang, R. M. Wolf, J. W. Caldwell, P. A. Kollman and D. A. Case, *J. Comput. Chem.*, 2004, **25**, 1157–1174.
17 T. Linder, B. L. de Groot and A. Stary-Weinzinger, *PLoS Comput. Biol.*, 2013, **9**, e1003058.
18 A. Stary, S. J. Wacker, L. Boukharta, U. Zachariae, Y. Karimi-Nejad, J. Aqvist, G. Vriend and B. L. de Groot, *ChemMedChem*, 2010, **5**, 455–467.
19 K.-M. Thai, A. Windisch, D. Stork, A. Weinzinger, A. Schiesaro, R. H. Guy, E. N. Timin, S. Hering and G. F. Ecker, *ChemMedChem*, 2010, **5**, 436–442.
20 P. Schmidtke, M. Ciantar, I. Theret and P. Ducrot, *J. Chem. Inf. Model.*, 2014, **54**, 2320–2333.
21 M. Holmgren, P. L. Smith and G. Yellen, *J. Gen. Physiol.*, 1997, **109**, 527–535.
22 U. Zachariae, F. Giordanetto and A. G. Leach, *J. Med. Chem.*, 2009, **52**, 4266–4276.
23 C. E. Dempsey, D. Wright, C. K. Colenso, R. B. Sessions and J. C. Hancox, *J. Chem. Inf. Model.*, 2014, **54**, 601–612.
24 V. Garg, A. Stary-Weinzinger, F. Sachse and M. C. Sanguinetti, *Mol. Pharmacol.*, 2011, **80**, 630–637.
25 M. J. Lenaeus, D. Burdette, T. Wagner, P. J. Focia and A. Gross, *Biochemistry (Mosc.)*, 2014, **53**, 5365–5373.
26 I. Baburin, S. Beyl and S. Hering, *Pflugers Arch.*, 2006, **453(1)**, 117–23.
27 M. J. Frisch, G. W. Trucks, H. B. Schlegel, G. E. Scuseria, M. A. Robb, J. R. Cheeseman, G. Scalmani, V. Barone, B. Menucci, G. A. Petersson, H. Nakatsuji, M. Caricato, X. Li, H. P. Hratchian, A. F. Izmaylov, J. Bloino, G. Zheng, J. L. Sonnenberg, M. Hada, M. Ehara, K. Toyota, R. Fukuda, J. Hasegawa, M. Ishida, T. Nakajima, Y. Honda, O. Kitao, H. Nakai, T. Vreven, J. A. Jr. Montgomery, J. E. Peralta, F. Ogliaro, M. Bearpark, J. J. Heyd, E. Brothers, K. N. Kudin, V. N. Staroverov, R. Kobayashi, J. Normand, K. Raghavachari, A. Rendell, J. C. Burant, S. S. Iyengar, J. Tomasi, M. Cossi, N. Rega, J. M. Millam, M. Klene, J. E. Knox, J. B. Cross, V. Bakken, C. Adamo, J. Jaramillo, R. Gomperts, R. E. Stratmann, O. Yazyev, A. J. Austin, R. Cammi, C. Pomelli, J. W. Ochterski, R. L. Martin, K. Morokuma, V. G. Zakrzewski, G. A. Voth, P. Salvador, J. J. Dannenberg, S. Dapprich, A. D. Daniels, Ö. Farkas, J. B. Foresman, J. V. Ortiz, J. Cioslowski and D. J. Fox, GAUSSIAN 09, Revision A.1 Gaussian, Inc., Wallingford CT, 2009.
28 D. A. Case, T. A. Darden, T. E. Cheatham, C. L. Simmerling and J. Wang, Amber 11, University of California, San Francisco, 2010.
29 B. Webb and A. Sali, *Curr Protoc Bioinformatics*., 2014, **47**, 5.6.1-5.6.32.
30 Y. X. Jiang, A. Lee, J. Y. Chen, V. Ruta, M. Cadene, B. T. Chait and R. MacKinnon, *Nature*, 2003, **423**, 33–41.
31 S. Y. Lee, A. Lee, J.Y. Chen and R. MacKinnon, Proc. Natl. Acad. Sci. U.S.A., 2005, **102**, 15441–15446.
32 V. Tsodikov, M. T. Record and Y. V. Sergeev, *J Comput Chem.*, 2002, **23(6)**, 600–609.

The hERG cavity can trap very bulky compounds, without perturbing normal gate closure